Inorganica Chimica Acta, 57 (1982) 79–86

Chemical Applications of Topology and Group Theory. 12. Post-transition Element Clusters with Particular Emphasis on Nine Vertex Systems

R. BRUCE KING

Department of Chemistry, University of Georgia, Athens, Ga. 30602, U.S.A.

Received April 23, 1981

The previously reported graph theoretical model of aromaticity in two and three dimensions is used to treat homoatomic post-transition element ions containing germanium, tin, lead, antimony, bismuth, selenium, and tellurium. Localized bonding models are sufficient to treat three and seven vertex systems as well as 12 skeletal electron trigonal bipyramidal five vertex systems such as Sn_5^{2-}, Pb_5^{2-}, and Bi_5^{3+}. The squares Bi_4^{2-}, Se_4^{2+}, and Te_4^{2+} are two-dimensional aromatic systems completely analogous to $C_4H_4^{2-}$. Most interesting are the nine vertex systems which can be classified into the following three types: (1) The 20 skeletal electron Ge_9^{2-} system which adopts the tricapped trigonal prismatic configuration expected for a closo 2n + 2 skeletal electron system; (2) The 22 skeletal electron Ge_9^{4-}, Sn_9^{4-}, and Pb_9^{4-} systems which adopt the capped square antiprismatic configuration with one non-triangular face expected for a nido 2n + 4 skeletal electron system; (3) The 22 skeletal electron Bi_9^{5+} system which is 'anomalous' since it adopts the closo deltahedral tricapped trigonal prismatic configuration rather than the nido capped square antiprismatic configuration expected for a 2n + 4 skeletal electron system. However, the tricapped trigonal prism in the 22 electron Bi_9^{5+} system is more 'elongated' than the tricapped trigonal prisms in 20 skeletal electron nine vertex clusters such as $B_9H_9^{2-}$, $B_7H_7C_2(CH_3)_2$, and Ge_9^{2-}. Detailed graph theoretical calculations show that such elongation of the tricapped trigonal prism can lead to incomplete overlap of the nine unique internal orbitals which generates the two core bonding orbitals required to accommodate the four core bonding electrons in a 2n + 4 skeletal electron system. These calculations also provide an illustration of a graph splitting algorithm for the symmetry factoring of graph characteristic polynomials.

Introduction

For more than 100 years certain planar polygonal species, of which benzene is the classical example [2, 3], have been recognized to have exceptional stability, conveniently known as 'aromaticity'. Within the past two decades more recently discovered three-dimensional polyhedral cage compounds have also been recognized to have exceptional stability: examples of the latter class of compounds include the dianions $B_nH_n^{2-}$ ($6 \leqslant n \leqslant 12$) [4, 5], carboranes $C_2B_{n-2}H_n$ ($6 \leqslant n \leqslant 12$) [6], and metal clusters of certain types [7, 8]. These observations lead naturally to the concepts of two-dimensional and three-dimensional aromaticity [9, 10]. Extensive theoretical work has been done with the objective of understanding the three-dimensional aromatic systems [10–14]. Furthermore, a recently reported [10] graph theoretical model of three-dimensional aromaticity demonstrates the close relationship between aromaticity in two and three dimensions.

Both experimental and theoretical observations indicate the following characteristics of structures exhibiting the full global delocalization conveniently known as three-dimensional aromaticity: (1) A structure based on a polyhedron with only triangular faces conveniently called a 'deltahedron'; (2) The absence of tetrahedral chambers in the deltahedron; (3) The presence of 2n + 2 skeletal electrons where n is the number of vertices of the deltahedron. If triangular faces or circuits are regarded as closed surfaces and faces or circuits with more than three sides are regarded as holes, then structures exhibiting three-dimensional aromaticity are topologically homeomorphic [15] to the sphere in the same sense that structures exhibiting two-dimensional aromaticity are homeomorphic to the circle.

The work described in this paper arose from a consideration of possible vertex atoms for polyhedral molecules exhibiting three-dimensional aromaticity. The motivation for the original development of the theory of three-dimensional aromatic systems was the explanation of the chemistry of certain polyhedral species having vertices consisting of carbon (RC), boron (RB), and/or middle transition metal moieties (*i.e.*, $M(CO)_n$, MC_5H_5 units involving the transition

metals whose chemistry is primarily influenced by the tendency to acquire the favored rare gas electronic configuration). However, polyhedral species are not necessarily confined to these regions of the periodic table. For example, numerous homopolyatomic ions of the post-transition elements are now known [16]. This paper examines the bonding in such ions with particular emphasis on possible candidates for systems exhibiting three-dimensional aromaticity. In this connection the nine vertex systems prove to be of particular interest since certain limiting conditions of the previously reported [10] model of three-dimensional aromaticity become apparent for the first time. In general the detailed discussion in this paper will be limited to species whose structures have been unambiguously determined by X-ray diffraction in order to have the theory on as firm a foundation as possible.

Background

The topology of a molecule will be represented by a graph in which the vertices correspond to atoms and the edges to chemical interactions of a given type. In the case of a polyhedral species such a graph need not correspond to the 1-skeleton [17] of the polyhedron since the chemical interactions of interest need not (and in this work will not) be directed along the edges of the polyhedron.

The methods for separating the topological effects from the usual secular equation have been discussed in detail elsewhere [10, 18–21]. Thus consider the usual secular equation

$$|\mathbf{H} - \mathbf{ES}| = 0 \tag{1}$$

in which the energy and overlap matrices can be resolved as follows:

$$\mathbf{H} = \alpha\mathbf{I} + \beta\mathbf{A} \tag{2a}$$

$$\mathbf{S} = \mathbf{I} + \mathbf{SA} \tag{2b}$$

In equations 2a and 2b **I** is the unit matrix, α and β are the Hückel Coulomb and resonance integrals, respectively, and **A** is the adjacency matrix [22] of the graph representing the topology of the system defined as follows:

$$A_{ij} = \begin{cases} 0 \text{ if } i = j \\ 1 \text{ if } i \text{ and } j \text{ are connected by an edge} \\ 0 \text{ if } i \text{ and } j \text{ are not connected by an edge} \end{cases} \tag{3}$$

The energy levels of the system can be calculated from the following equation:

$$E = \frac{\alpha + x\beta}{1 + xS} \tag{4}$$

In this equation x corresponds to the eigenvalues of **A** defined as follows:

$$|\mathbf{A} - x\mathbf{I}| = 0 \tag{5}$$

This treatment thus shows how the energy levels of the system can be determined from the eigenvalues of the adjacency matrix of the graph representing the topology of the relevant chemical interactions.

A characteristic feature of both two- and three-dimensional aromaticity is the involvement of three orbitals of each vertex atom (conveniently known as *internal* orbitals) in the bonding associated with the aromatic skeleton. These three internal orbitals can be partitioned into a pair of twin internal orbitals and a third unique internal orbital. The twin internal orbitals (approximate sp^2 hybrids in the two-dimensional systems and p orbitals in the three-dimensional systems) overlap pairwise to form the surface bonding (this is the σ-bonding in the two-dimensional systems). This surface bonding generates equal numbers of bonding and antibonding orbitals (n orbitals of each type for a system with n vertices). The unique internal orbitals overlap to participate in bonding that is characteristic of the type of aromatic system involved. The graph representing the overlap of the unique internal orbitals is the one that is used to calculate the eigenvalues (eqns. 3 and 5) and from them the energy levels (eqn. 4). In the case of the two-dimensional aromatic systems the overlap between the unique internal orbitals (*i.e.*, the p orbitals) has the topology of the cyclic graphs C_n which are isomorphic to the corresponding regular polygons. This overlap corresponds to the π-bonding in these systems. In the case of the three-dimensional aromatic systems the overlap between the unique internal orbitals (approximate sp hybrids) occurs in the core of the deltahedron and has the topology of the corresponding complete graphs K_n [23] in which there is an edge between every possible vertex pair. This overlap thus represents an n-center core bond. Since the complete graphs K_n have only one positive eigenvalue for any value of n, stable three-dimensional aromatic systems have 2n + 2 skeletal electrons in which the 2n electrons fill the n bonding surface molecular orbitals and the remaining 2 electrons fill the single bonding core molecular orbital. These relationships are summarized in Table I. Additional details of this graph theoretical bonding model for deltahedral molecules are given in the earlier paper [10] including extensions to polyhedra with some non-triangular faces (the electron rich systems with more than 2n + 2 skeletal electrons) and polyhedra with tetrahedral chambers (the electron poor systems with less than 2n + 2 skeletal electrons).

There are several implications of this bonding model for three-dimensional aromatic systems with n vertices.

TABLE I. Comparison of the Bonding in Two-Dimensional and Three-Dimensional Aromatic Systems with n Vertices.

	Two-Dimensional Aromatic Systems (Polygons)	Three-Dimensional Aromatic Systems (Deltahedra)
A) Orbital Hybridizations		
External[a]	sp^2	sp
Twin Internal	sp^2	p
Unique Internal	p	sp
B) Orbital Interactions		
1) Twin Internal		
a) Bonding type	σ	Surface
b) Interaction Topology	nK_2	nK_2
c) Number of bonding orbitals	n	n
d) Number of bonding electrons	2n	2n
2) Unique Internal		
a) Bonding type	π	core
b) Interaction Topology	C_n	K_n
c) Number of bonding orbitals	odd (2k + 1)	1
d) Number of bonding electrons	4k + 2	2

[a]For clarity the obvious d orbital participation in transition metal and post-transition element vertices is excluded.

(1) The overlap of the n unique internal orbitals with the topology of the complete graph K_n to form an n center core bond may be hard to visualize since the graphs K_n for $n \geqslant 5$ are non-planar by Kuratowski's theorem [24] and therefore cannot correspond to the 1-skeleton [17] of a polyhedron realizable in three-dimensional space. However, the overlap of these unique internal orbitals does *not* occur along the edges of the deltahedron or those of any other three-dimensional polyhedron. For this reason, the topology of the overlap of the unique internal orbitals in the core bonding of a deltahedral cluster need not correspond to a graph representing a 1-skeleton of a three-dimensional polyhedron. The only implication of the K_n graph representation of the bonding topology of the unique internal orbitals is that the deltahedron is topologically homeomorphic [15] to the sphere.

(2) The precise topology of the deltahedron (*i.e.* what pairs of vertices are connected directly by edges) thus does not affect directly the graph (namely K_n) representing the overlap between the unique internal orbitals. However, the detailed structure of the deltahedron relates directly to the following points: (a) The presence of the Hamiltonian circuits [10, 25] required for realizability of the pairwise surface bonding of the twin internal orbitals is assured by theorems [26] relating the presence of Hamiltonian circuits to relationships between numbers of vertices and edges which are satisfied for all deltahedra; (b) The homeomorphism to the sphere required for realizability of the n-center core bonding is assured by the absence of non-triangular faces in deltahedra.

(3) The equality of the interactions between all possible pairs of unique internal orbitals required by the K_n model for the core bonding is obviously a very crude assumption since in any deltahedron with five or more vertices all pairwise relationships of the vertices are not equivalent. Thus the *cis* and *trans* vertex pairs in an octahedral cluster such as $B_6H_6^{2-}$ are clearly different. However, the single eigenvalue of the K_n graph is so strongly positive that severe inequalities in the different vertex pair relationships are required before the spectrum of the graph representing precisely the unique internal orbital overlap contains more than one positive eigenvalue. In other words, the graph theoretical model for three-dimensional aromaticity has a high tolerance for distortion before it ceases to predict the proper number of skeletal electrons. The nine vertex post-transition element clusters examined in this paper are significant in that they show how much a deltahedron can be distorted before the core bonding will generate more than the single bonding molecular orbital implied by the K_n topology.

Homoatomic Post-Transition Element Clusters with Less than Nine Vertices

This paper surveys the bonding in homoatomic clusters of the heavier post-transition elements of

groups IV, V, and VI (*i.e.* germanium, antimony, selenium, and their heavier congeners). Such clusters are always ionic. The cationic species generally arise by reduction of the chlorides with the free element in acidic chlorometallate melts, mainly $AlCl_4^-$ [16]. They are isolated as salts of chlorometallate anions. The anionic species [27, 28] arise by reduction of the free element with an alkali metal in liquid ammonia or an amine and can be isolated by complexation with cryptate [29] ligands. In contrast to the polyhedral boranes, carboranes, and metal clusters, none of the homoatomic post-transition element clusters considered in this paper contains any 'external' groups bonded to the cluster atoms. In other words the clusters have the simple stoichiometry E_n^z where E is the post-transition element, n is the number of atoms of the element in the cluster, and z is the charge on the cluster.

The rules for counting the number of skeletal electrons contributed by each vertex atom can be adapted to vertices consisting of post-transition elements lacking external groups by the following procedure:

(1) The post-transition elements under consideration have a total of nine valence orbitals, namely one s, three p, and five d orbitals.

(2) The post-transition elements (in their zero oxidation states) have a total of 10 + G valence electrons, where G is the group of the periodic table where the post-transition element is located. Thus germanium, tin, and lead have 10 + 4 = 14 valence electrons, antimony and bismuth have 10 + 5 = 15 valence electrons, and selenium and tellurium have 10 + 6 = 16 valence electrons.

(3) If the clusters have either two- or three-dimensional aromaticity, three orbitals of each vertex atom will be required for the internal orbitals (two twin internal orbitals and one unique internal orbital). This leaves six external orbitals. Each external orbital must be filled with an electron pair thereby consuming 2 × 6 = 12 electrons from each vertex atom in systems lacking external groups such as those under consideration.

(4) The number of skeletal electrons contributed by each vertex atom through its three internal orbitals must therefore be 10 + G − 12 = G − 2. Application of this rule to the post-transition elements of interest indicates that the group IV elements germanium, tin, and lead contribute 2 skeletal electrons, the group V elements antimony and bismuth contribute 3 skeletal electrons, and the group VI elements selenium and tellurium contribute 4 skeletal electrons when they occur as vertices in two- or three-dimensional aromatic systems. Thus the group IV elements Ge, Sn, and Pb are isoelectronic with BH, $Fe(CO)_3$, and C_5H_5Co vertices and the group V elements Sb and Bi are isoelectronic with CH, $Co(CO)_3$, and C_5H_5Ni vertices in cluster compounds. It therefore seems reasonable that rules for the bonding in polyhedral boranes, carboranes, and metal clusters might also apply to post-transition element clusters having group IV and V elements as vertices.

The following homoatomic post-transition element clusters have been characterized by X-ray crystallography:

(1) Three-atom clusters:

The three-atom clusters Hg_3^{2+} [30] and Te_3^{2-} [31] are open systems containing no bonding features of interest in the context of this paper. For example, the species Te_3^{2-} is isoelectronic with tellurium(II) halides TeX_2.

(2) Four-atom clusters:

A series of square four-atom clusters are known which have 14 skeletal electrons in all cases. Specific examples of such clusters are Bi_4^{2-} [32], Se_4^{2+} [33], and Te_4^{2+} [34]. These species are isoelectronic with the cyclobutadiene dianion $C_4H_4^{2-}$ and are therefore two-dimensional aromatic systems. In these systems eight of the 14 skeletal electrons are used for localized two-electron σ-bonds along the four edges of the square and the remaining six skeletal electrons from a delocalized 6π electron system similar to that in the cyclopentadienide ion or benzene.

(3) Five-atom clusters:

A series of trigonal bipyramidal clusters are known which have 12 skeletal electrons in all cases. Specific examples of such clusters are Sn_5^{2-} [35], Pb_5^{2-} [35], and Bi_5^{3+} [16]. These species are isoelectronic with the known [36] carborane $C_2B_3H_5$ and its derivatives as well as the unknown $B_5H_5^{2-}$ and thus are expected to have similar bonding.

Some specific comments about the bonding in these trigonal bipyramidal species are in order since most of the literature on this topic can be misleading. The original assumption applied to the boron polyhedra [4–6] was that the five-vertex species $C_2B_3H_5$ and $B_5H_5^{2-}$ would be stabilized by delocalization in a manner similar to their higher analogues $C_2B_{n-2}H_n$ ($6 \leqslant n \leqslant 12$) and $B_nH_n^{2-}$. However, persistent failures to prepare $B_5H_5^{2-}$ suggests that this species is not stabilized to the same extent as its higher analogues. Furthermore, a recent survey of carborane chemistry [36] suggests that $C_2B_3H_5$ is significantly more chemically reactive than the higher carboranes $C_2B_{n-2}H_n$ ($6 \leqslant n \leqslant 12$). The compelling conclusion from these experimental observations is that trigonal bipyramidal clusters are not stabilized by delocalization in the same manner as deltahedral clusters with six or more vertices.

The lack of delocalization in trigonal bipyramidal clusters is consistent with some recent theoretical work. Thus in Aihara's model of three-dimensional aromaticity [9] the trigonal bipyramidal system as examplified by $B_5H_5^{2-}$ has no resonance energy

just like the B_4H_4 tetrahedral system. Furthermore, our previous analysis of three-dimensional aromaticity [10] leads to the conclusion that tetrahedral systems have edge localized bonding and that similar localized bonding will prevail in any tetrahedral chambers of more complex polyhedra. Since a trigonal bipyramid consists of two tetrahedral chambers with a face in common, this theory suggests that trigonal bipyramidal clusters have localized bonding.

In view of these considerations the bonding in the 12 skeletal electron systems with trigonal bipyramidal geometry (*e.g.* $C_2B_3H_5$, Sn_5^{2-}, Pb_5^{2-}, and Bi_5^{3+}) can be represented by six localized two-electron bonds along the edges of a $K_{2,3}$ bipartite graph, which was recently introduced in connection with a discussion of the stereochemical non-rigidity of five-coordinate systems [37]. Thus the carborane $C_2B_3H_5$ can be represented by structure I in which the two carbon atoms are the normal tetrahedral sp^3 type and the boron atoms are the planar sp^2 type found in trialkylboranes. Analogous localized bonding models are possible for the other 12 skeletal electron trigonal bipyramidal species mentioned above.

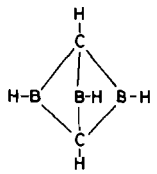

I

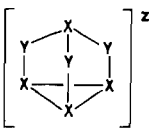

II

(4) Seven-atom clusters:

The one well-characterized post-transition element homoatomic seven-atom cluster is Sb_7^{3-} [38] which is isoelectronic and isostructural with P_4S_3. These species have structures II (X = Y = Sb, z = −3 for Sb_7^{3-}, and X = P, Y = S, z = 0 for P_4S_3) which can be formulated with nine two-electron localized bonds along the edges. Note that in this localized cluster the Y atoms may be regarded as having two internal and seven external orbitals rather than the three internal and six external orbitals required for the delocalized clusters.

The Nine Vertex Clusters

The preceding section shows that none of the well-characterized post-transition element clusters with less than nine vertices have three-dimensional aromaticity although the square Bi_4^{2-}, Se_4^{2+}, and Te_4^{2+} are clear examples of two-dimensional aromatic systems. However, the nine vertex systems introduce a variety of new features which extend the previous ideas [10] on three-dimensional aromaticity.

The following two nine-vertex polyhedra are involved in the chemistry of the nine atom family [39]:

(1) The 4,4,4-tricapped trigonal prism (structure III) with 21 edges and 14 faces, all of which are triangles. This polyhedron is therefore a deltahedron which should correspond to a closo system with 2n + 2 = 20 skeletal electrons.

(2) The 4-capped square antiprism (structure IV) with 20 edges and 13 faces. One of the faces is square and the remaining 12 faces are triangles. This polyhedron therefore has one hole (the square face) and thus should correspond to an 'electron-rich' [10] nido system with 2n + 4 = 22 skeletal electrons.

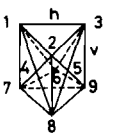

III

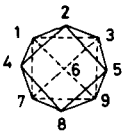

IV

The nine-vertex homoatomic clusters of the post-transition elements fall into the following three categories:

(1) The anion Ge_9^{2-} which has been shown to have a 4,4,4-tricapped trigonal prismatic structure [40]. Since this system has 9 (4 − 2) + 2 = 20 = 2n + 2 skeletal electrons, a closo deltahedral structure is expected for Ge_9^{2-} in accord with what has been found.

(2) The anions E_9^{4-} (E = Ge [40], Sn [41], and Pb [41]) which have been shown by X-ray diffraction to have 4-capped square antiprismatic structures. Since these systems have 9 (4 − 2) + 4 = 22 = 2n + 4 skeletal electrons, a nido polyhedral structure having one face with more than three edges is expected in accord with what has been found.

(3) The cation Bi_9^{5+} which has been shown [42] to have a 4,4,4-tricapped trigonal prismatic structure which is the closed deltahedron expected for a system with 2n + 2 = 20 skeletal electrons. However, the Bi_9^{5+} system has 9 (5 − 2) − 5 = 22 skeletal electrons leading to the prediction of a nido polyhedron with one non-triangular face in contradiction to what has been found.

The Bi_9^{5+} system is thus a case where the simple skeletal electron counting rules for three-dimensional aromatic systems [10–14] lead to the prediction of an incorrect structure. This section examines possible reasons for this discrepancy.

An initial clue to this anomaly is provided by a detailed examination of the geometries of the various 4,4,4-tricapped trigonal prismatic clusters.

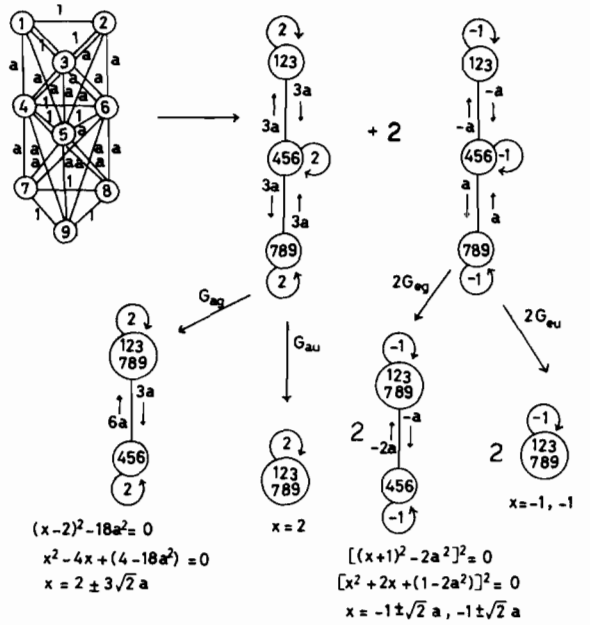

Fig. 1. Application of the graph splitting algorithm for the symmetry factoring of the ninth degree characteristic equation of the graph representing the overlap of the unique internal orbitals in Bi_9^{5+}.

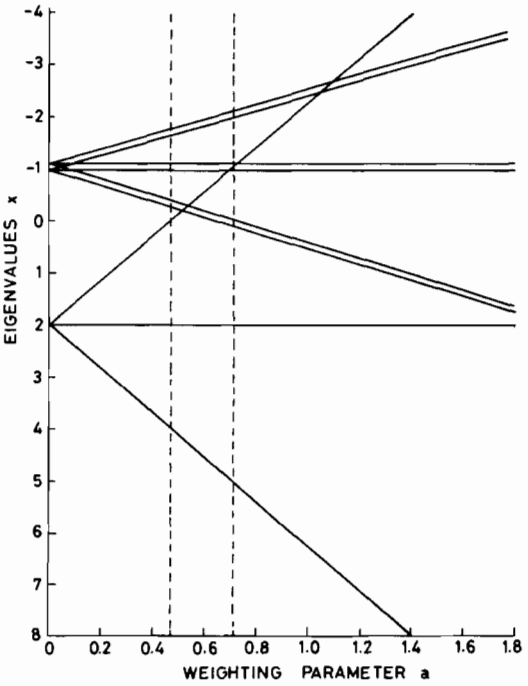

Fig. 2. Plot of the eigenvalues of the nine vertex graph in Fig. 1 as a function of the weighting parameter a representing the ratio of intertriad interactions to intratriad interactions. The doubly degenerate eigenvalues are represented by a pair of closely spaced lines. The vertical dashed lines enclose the range of the weighting parameter ($0.47 < a < 0.71$) where two positive eigenvalues are found. Note that in Fig. 2 the positive eigenvalues are in the lower part of the ordinate and the negative eigenvalues are in the upper part of the ordinate in accord with the energies of the corresponding molecular orbitals.

The ratio v/h of the prism 'height' v (*e.g.* edges 17, 28, or 39 in structure III) to the 'basal edge' h (*e.g.* edges 12, 23, 31, 78, 89 and 97 in structure III) [39] is particularly significant. Thus in the 20 skeletal electron systems Ge_9^{2-} (1.03), $B_9H_9^{2-}$ (0.97), and $B_7H_7C_2(CH_3)_2$ (0.90) the v/h ratio (given in parentheses) is appreciably smaller than that in the 22 skeletal electron system Bi_9^{5+} (1.15). This suggests that the extra skeletal electron pair in the Bi_9^{5+} system arises because its tricapped trigonal prism is so stretched out that each of the nine unique internal orbitals of the vertex atoms cannot overlap with every other such orbital as represented topologically by the K_9 complete graph. More specifically the unique internal orbitals of the three atoms of the 'top' triangular face of the tricapped trigonal prism (atoms 1, 2, and 3 in structure III) cannot overlap any more with the unique internal orbitals of the three atoms of the 'bottom' triangular face (atoms 7, 8, and 9 in structure III). The eigenvalue spectrum of this 'revised' graph representing 'incomplete' overlap of the nine unique internal orbitals will now be calculated in order to test this hypothesis.

The relevant graph to represent the interactions of the nine unique internal orbitals in the stretched out tricapped trigonal prism in Bi_9^{5+} is depicted in Fig. 1. This graph may be regarded as two fused K_6 graphs, one involving the triad of 'top' triangle atoms 1, 2, and 3, as well as the triad of capping atoms 4, 5, and 6, and the other involving the triad of 'bottom' triangle atoms 7, 8, and 9 as well as the triad 4, 5, and 6. Thus the vertices 4, 5, and 6 are common to both K_6 graphs and have degree 8 whereas the remaining six vertices are only contained in a single K_6 graph and therefore have degrees of only 5. Furthermore, a variable parameter a is introduced which represents the ratios between the intratriad interactions (*i.e.* those within the triads 123, 456, and 789) and the intertriad interactions (*i.e.* those between the triads 123 and 456 and between the triads 456 and 789). Thus the nine edges 12, 23, 31, 45, 46, 64, 78, 89, and 97 are given weight 1 and the remaining 18 edges 14, 15, 16, 24, 25, 26, 34, 35, 36, 47, 57, 67, 48, 58, 68, 49, 59, and 69 are given weight a. The effective D_{3h} symmetry of this graph is then used to factor its ninth degree characteristic polynomial into six factors. The graph splitting algorithm used to effect this factoring has been reported elsewhere [43] and the details of this particular case are given in Fig. 1. Note that in this case the symmetry factoring process involves two stages:

(1) Use of the three-fold rotation axis to split the original connected graph into a disconnected graph with three components of three vertices each. One of these components is unique and is designated as G_a. The remaining two components are identical and are designated as G_e.

(2) Use of the planes of symmetry in both the G_a and G_e components to factor each of the three-vertex connected components into a single vertex (G_{au} and G_{eu}) and a pair of connected vertices (G_{ag} and G_{eg}).

The net result of this symmetry factoring process is the splitting of the original connected graph with nine vertices into a disconnected graph with six components so that the eigenvalues of the disconnected graph are the same as those of the original connected graph. As a consequence of this procedure only quadratic and linear equations need to be solved in order to determine all nine eigenvalues of the original connected graph. It is therefore feasible to express solutions of these equations in terms of the edge weighting parameter a using algebra no more complicated than the 'quadratic formula'.

The number of positive eigenvalues of the graph in Fig. 1 is directly related to the number of bonding orbitals arising from overlap of the nine unique internal orbitals and thus to the number of skeletal electrons in the nine vertex system. Figure 2 plots the eigenvalues of this nine vertex graph as a function of the weighting parameter a. For values of a less than 0.47 (*i.e.*, $\sqrt{2}/3$) the graph has three positive eigenvalues, for values of a between 0.47 and 0.71 (*i.e.*, $\sqrt{2}/2$) the graph has two positive eigenvalues, and for values greater than 0.71 the graph has four positive eigenvalues. Thus in the range $0.47 < a < 0.71$ the graph in Fig. 1 has the two positive eigenvalues required for the generation of two bonding orbitals from overlap of the nine unique internal orbitals. In this range the core bonding of the nine-vertex polyhedron requires 4 skeletal electrons which when added to the 2n = 18 skeletal electrons required for the surface bonding in a nine vertex polyhedron leads to the 22 skeletal electrons found in Bi_9^{5+}. We thus see how stretching out the 4,4,4-tricapped trigonal prism deltahedron can destroy the perfect nine-center bond of the unique internal orbitals so that an additional bonding pair of electrons is required. In other words a stretched out deltahedron with non-triangular faces can mimic in its electron count a nido polyhedron with a single non-triangular face.

The above treatment, although obviously very crude, shows how the ideal three-dimensional aromaticity model [10] can be modified to account for the extra skeletal electron pair in Bi_9^{5+} in a manner consistent with geometrical differences between the tricapped trigonal prism in Bi_9^{5+} and corresponding deltahedra in the other nine-vertex systems (*e.g.* $B_9H_9^{2-}$, $B_7H_7C_2(CH_3)_2$, and Ge_9^{2-} which have the 2n + 2 = 20 skeletal electrons required by the ideal three-dimensional aromaticity model [10]. A related question is why the 22 skeletal electron Bi_9^{5+} system does not instead acquire the 4-capped square antiprism geometry of the 22 electron E_9^{4-} systems (E = Ge, Sn, and Pb). In this connection the following two points seem relevant:

(1) Guggenberger and Muetterties [39] have shown that for nine vertex systems (both M_9 clusters and ML_9 coordination complexes) the tricapped trigonal prism III is of lower energy than the capped square antiprism IV.

(2) The high formal positive charge on the Bi_9^{5+} system relative to the high formal negative charge on the E_9^{4-} systems makes the unique internal orbitals in the Bi_9^{5+} system less diffuse than those in the isoelectronic E_9^{4-} systems. The range of overlap of the unique internal orbitals in Bi_9^{5+} is therefore much more restricted than that of the unique internal orbitals in the E_9^{4-} anions.

These points suggest that the types of geometric distortions in polyhedral molecules to accommodate electron-rich systems (*i.e.* those with more than 2n + 2 skeletal electrons) depend upon the electron density of the vertex atoms. Most electron-rich systems prefer to adopt the structures based on polyhedra with one or more non-triangular faces as exemplified by the nido and arachno compounds. However, systems rich in skeletal electrons but with a low electron density on the vertex atoms as exemplified by Bi_9^{5+} may prefer to adopt deltahedral structures but with distortions to prevent complete overlap of all of the unique internal orbitals. This paper shows that the existing theoretical models can accommodate such possibilities. Further work on the structures of other post-transition element homoatomic *cations* of high nuclearity is needed to establish the generality of such behavior. A particularly interesting reported [16] system is Bi_8^{2+} for which a square antiprismatic structure has been suggested but not proven. The Bi_8^{2+} system has $8(5-2)-2 = 22 = 2n + 6$ skeletal electrons. Since a square antiprism has *three* positive eigenvalues (namely [43] 4, $\sqrt{2}$, and $\sqrt{2}$), a square antiprismatic structure for Bi_8^{2+} can be rationalized by a three-dimensional aromaticity model modified so that the overlap of the eight unique internal orbitals has the topology of the square antiprism rather than one or more fused or disjoint K_n graphs.

Finally a molecular orbital study in 1964 by Corbett and Rundle [44] on Bi_9^{5+} should be mentioned. These authors were able to rationalize the 22 skeletal electrons of Bi_9^{5+}. However, the additional points discussed in the present paper are not apparent from their much earlier work largely because very little was known about nine-vertex clusters or even possible polyhedra for such systems in 1964.

Summary

This paper shows that simple conventional models of two- and three-dimensional aromaticity can be applied to post-transition element clusters to provide reasonable explanations of their structures and electron counts. Thus there are no fundamental differences in the structure and bonding of post-transition element clusters as compared with polyhedral boranes, carboranes, and middle transition metal clusters. However, the specific post-transition element clusters which have been structurally characterized permit the extension of known cluster bonding models in the following directions:

(1) Additional examples of 12 skeletal electron trigonal bipyramidal clusters in which edge localized bonding models are satisfactory.

(2) The first case in which incomplete overlap of the unique internal orbitals in a deltahedron appears to occur in a system isoelectronic with a nido system (*i.e.*, Bi_9^{5+}). This suggests the following areas for further experimental work in the field of post-transition element clusters:

(1) The synthesis of additional cationic species which might be conceivable candidates for three-dimensional systems exhibiting incomplete overlap of unique internal orbitals.

(2) The combination of post-transition element cluster chemistry with transition metal organometallic chemistry to synthesize new types of clusters containing both post-transition element and transition metal organometallic vertices. In this connection some iron carbonyl derivatives of tin, lead, antimony, bismuth, *etc.*, prepared by Hieber, Gruber, and Lux in 1959 [45] and whose structures are not yet understood may prove to be compounds of this type.

Acknowledgements

The author acknowledges a helfpul discussion with Prof. J. D. Corbett of Iowa State University during a visit there in October, 1979, which focussed his attention onto the anomalies of the Bi_9^{5+} system. The author also acknowledges financial support by the National Science Foundation under Grant CHE-77-15991.

References

1 For part 11 of this series, see R. B. King, *Inorg. Chim. Acta, 49,* 237 (1981).
2 E. Hückel, *Z. Physik, 70,* 204 (1931).
3 M. J. S. Dewar, 'The Molecular Orbital Theory of Organic Chemistry', McGraw–Hill, New York 1969, Chapter 5.
4 E. L. Muetterties and W. H. Knoth, 'Polyhedral Boranes', Marcel Dekker, New York, 1968.
5 E. L. Muetterties, Ed., 'Boron Hydride Chemistry', Academic Press, New York, 1975.
6 R. N. Grimes, 'Carboranes', Academic Press, New York, 1970.
7 R. B. King, *Prog. Inorg. Chem., 15,* 287 (1972).
8 P. Chini, G. Longoni and V. G. Albano, *Advan. Organometal. Chem., 14,* 285 (1976).
9 J. -i. Aihara, *J. Am. Chem. Soc., 100,* 3339 (1978).
10 R. B. King and D. H. Rouvray, *J. Am. Chem. Soc., 99,* 7834 (1977).
11 K. Wade, *Chem. Comm.,* 792 (1971).
12 R. Rudolph and W. R. Pretzer, *Inorg. Chem., 11,* 1974 (1972).
13 R. N. Grimes, *Ann. N.Y. Acad. Sci., 239,* 180 (1974).
14 K. Wade, *Advan. Inorg. Chem. Radiochem., 18,* 1 (1976).
15 M. J. Mansfield, 'Introduction to Topology', Van Nostrand, Princeton, New Jersey, 1963, Chapter 3.
16 J. D. Corbett, *Prog. Inorg. Chem., 21,* 129 (1976).
17 B. Grünbaum, 'Convex Polytopes', Interscience, New York, 1967.
18 K. Ruedenberg, *J. Chem. Phys., 22,* 1878 (1954).
19 H. H. Schmidtke, *Coord. Chem. Rev., 2,* 3 (1967).
20 H. H. Schmidtke, *J. Chem. Phys., 45,* 3920 (1966).
21 I. Gutman and N. Trinajstić, *Topics Curr. Chem., 42,* 49 (1973).
22 N. L. Biggs, 'Algebraic Graph Theory', Cambridge University Press, London, 1974, p. 9.
23 R. J. Wilson, 'Introduction to Graph Theory', Oliver and Boyd, Edinburgh, 1972, p. 16.
24 K. Kuratowski, *Fundam. Math., 15,* 271 (1930).
25 M. Behzad and G. Chartrand, 'Introduction to the Theory of Graphs', Allyn and Bacon, Boston, Massachusetts, 1971, Chapter 11.
26 H. Sachs, 'Einführung in die Theorie der endlichen Graphen', Hanser, Munich, 1971, Chapter 2.
27 H. J. Emeléus and J. S. Anderson, 'Modern Aspects of Inorganic Chemistry', Third Edition, van Nostrand, New York, 1960, p. 512.
28 H. Schäfer, B. Eisenmann and W. Müller, *Angew. Chem. Int. Ed., 12,* 694 (1973).
29 J. M. Lehn, *Accts. Chem. Research, 11,* 49 (1978).
30 R. D. Ellison, H. A. Levy and K. W. Fung, *Inorg. Chem., 11,* 833 (1972).
31 A. Cisar and J. D. Corbett, *Inorg. Chem., 16,* 632 (1977).
32 A. Cisar and J. D. Corbett, *Inorg. Chem., 16,* 2482 (1977).
33 D. J. Prince, J. D. Corbett and B. Garbisch, *Inorg. Chem., 9,* 2731 (1970).
34 T. W. Couch, D. A. Lokken and J. D. Corbett, *Inorg. Chem., 11,* 357 (1972).
35 P. A. Edwards and J. D. Corbett, *Inorg. Chem., 16,* 903 (1977).
36 R. E. Williams, *Adv. Inorg. Chem. Radiochem., 18,* 67 (1976).
37 R. B. King, *Inorg. Chem., 16,* 1822 (1977).
38 D. G. Adolphson, J. D. Corbett and D. J. Merryman, *J. Am. Chem. Soc., 98,* 7234 (1976).
39 L. J. Guggenberger and E. L. Muetterties, *J. Am. Chem. Soc., 98,* 7221 (1976).
40 C. H. E. Belin, J. D. Corbett and A. Cisar, *J. Am. Chem. Soc., 99,* 7163 (1977).
41 J. D. Corbett and P. A. Edwards, *J. Am. Chem. Soc., 99,* 3313 (1977).
42 R. M. Friedman and J. D. Corbett, *Inorg. Chem., 12,* 1134 (1973).
43 R. B. King, *Theor. Chim. Acta, 44,* 223 (1977).
44 J. D. Corbett and R. E. Rundle, *Inorg. Chem., 3,* 1408 (1964).
45 W. Hieber, J. Gruber and F. Lux, *Z. anorg. allgem. Chem., 300,* 275 (1959).